Using Echo-State Networks to Reproduce Rare Events in Chaotic Systems

Anton Erofeev, Balasubramanya T. Nadiga, Ilya Timofeyev May 23, 2025

Abstract

We apply the Echo-State Networks to predict the time series and statistical properties of the competitive Lotka-Volterra model in the chaotic regime. In particular, we demonstrate that Echo-State Networks successfully learn the chaotic attractor of the competitive Lotka-Volterra model and reproduce histograms of dependent variables, including tails and rare events. We use the Generalized Extreme Value distribution to quantify the tail behavior.

Keywords: Echo-State Networks, competitive Lotka-Volterra, Chaotic time series, Rare events, Generalized Extreme Value distribution

1 Introduction

Machine learning has emerged as an alternative approach for solving partial differential equations, reproducing trajectories of dynamical systems, emulating statistical properties of chaotic systems, etc. Neural networks and deep learning play a particularly important role in developing new techniques for understanding and solving various dynamical systems.

Reservoir computing [15, 30] is a particular class of machine learning models; it utilizes a large recurrent network (reservoir), and only a linear output layer is trained to match the trajectory. Echo-State Networks refer to reservoirs that have the Echo-State Property (see e.g. [12, 13, 18, 3, 14, 8, 30]). There has been a considerable amount of research on Reservoir Computing (RC) and Echo-State Networks (ESNs). In particular, it has been demonstrated that ESNs are able to predict time series of nonlinear and chaotic models for several Lyapunov times (e.g. [21, 7, 11, 9, 19, 4, 5, 10, 22]). Moreover, starting with [21], it also has been demonstrated that Echo-State Networks are capable of reproducing the statistical properties of attractors in chaotic systems (see e.g. [20, 17, 28, 16, 1, 24, 26, 2]). Thus, it has been suggested that ESNs can be used to reproduce the statistical properties of chaotic attractors in high-dimensional complex systems, such as climate. However, it has been emphasized in the geophysical community that rare events can be particularly important for climate studies. Thus, our goal is to examine the applicability of ESN to a chaotic model with statistical behavior that is different from the "fast-decaying" tails of the Lorenz-63 and the Kuramoto-Sivashinsky models.

 $^{^*}$ University of Houston, aerofeev@uh.edu

[†]Los Alamos National Laboratory, balu@lanl.gov

[‡]University of Houston, itimofey@Central.uh.edu

In the context of dynamical systems, consider a flow map $\Phi_t(x): \mathbb{R}^d \to \mathbb{R}^d$ with the property $\Phi_{t+s} = \Phi_t \circ \Phi_s$ for any $s,t \geq 0$. For this paper, the flow map is generated by the numerical discretization of the 4-dimensional chaotic Lotka-Volterra equations. Predicting individual trajectories of dynamical systems is equivalent to learning the flow map itself. However, we can ask a different question regarding the long-term behavior of the ESN. In particular, assume that the flow map Φ_t admits an attractor with an ergodic invariant measure μ and thus, the long-time statistical behavior of trajectories is characterized by this invariant measure. However, since the metric for ESN's training focuses on individual trajectories, it is not obvious that ESN can learn the invariant measure μ . This question has been address previously, and it has been demonstrated numerically that ESN is capable of learning the invariant measure μ (e.g. [20, 17, 28, 16, 1, 24, 26, 2]) for several chaotic examples. In this paper, we focus our attention on how well ESN reproduces the "tails" of the invariant measure μ . Reproducing rare events is a notoriously difficult problem since the amount of training data is much smaller for these regions of phase space. Therefore, many Machine Learning and other types of reduced or surrogate models tend to reproduce bulk (e.g., means, variances, etc.) statistical properties correctly, but fail to accurately capture rare events.

We use Echo-State Networks to predict the dynamics of the four-dimensional competitive Lotka-Volterra equations [25, 27, 29] in the chaotic regime. In this regime, the invariant measure μ is characterized by sharp peaks and long, slowly-decaying tails. Thus, the statistical properties of the attractor of this system appear to be very different from the statistical properties of attractors in "classical" examples of chaos that have been used to study the applicability of ESNs, such as the Lorenz-63 and the Kuramoto-Sivashinsky models.

The main goal of this paper is to examine how well ESNs reproduce the statistical properties of the attractor in the 4D Lotka-Volterra model. We demonstrate that ESNs can learn the flow map Φ_t for several Lyapunov times, as well as the invariant measure μ . In particular, the emphasis in this paper is on rare events and reproducing the tails of marginal distributions. We use the generalized extreme value (GEV) distribution to quantify the performance of the ESN with respect to rare events. We also discuss the consequences of generalized synchronization for the ESN trained on the LV data.

2 Dynamic Equations and the Reservoir

Competitive Lotka-Volterra (LV) equations are a model of population dynamics for species competing for the same resource. It is a simple generalization of the classical 2D predator-prey model. We consider the 4D competitive Lotka-Volterra system

$$\frac{d}{dt}x_i = r_i x_i \left(1 - \sum_{j=0}^3 \alpha_{ij} x_j\right), \quad i = 0, \dots, 3$$

$$\tag{1}$$

with

$$r = \begin{pmatrix} 1 \\ 0.72 \\ 1.53 \\ 1.27 \end{pmatrix}, \qquad \alpha = \begin{pmatrix} 1 & 1.09 & 1.52 & 0 \\ 0 & 1 & 0.44 & 1.36 \\ 2.33 & 0 & 1 & 0.47 \\ 1.21 & 0.51 & 0.35 & 1 \end{pmatrix}.$$

The above model was investigated in [27, 29]. It was demonstrated that this model exhibits chaotic behavior for this set of parameters. Moreover, the chaotic behavior is robust to perturbations but

occurs for a relatively narrow set of parameters. The largest Lyapunov exponent for this model is $\lambda_{max} = 0.0203$. Thus, the Lyapunov time is approximately $T_{lyap} \approx 49.26$. In this paper, this model is integrated numerically using a fixed time-step Runge-Kutta 4th order method with the time-step $\delta t = 0.01$. We sample trajectories with the time-step $\Delta t = 2$. Thus, $\Delta t = 2$ is used as the ESN time-step for training and generating trajectories.

Reservoir. We use standard reservoir architecture. The equations for the reservoir are given by

$$r(t + \Delta t) = f(A r(t) + W_{in} x(t)), \tag{2}$$

where $r(t) \in \mathbb{R}^D$ is the reservoir state, $f = \tanh(x) : \mathbb{R}^D \to \mathbb{R}^D$ is the element-wise activation function. Matrices $A \in \mathbb{R}^{D \times D}$ and $W_{in} \in \mathbb{R}^{N \times D}$ (N = 4 is the dimension of the LV system) remain constant throughout the training process. During training, only the weights of the output layer, $W_{out} \in \mathbb{R}^{D \times N}$, are adjusted as linear regression weights for the reservoir states $r(t + \Delta t)$ to produce the output $x(t + \Delta t)$. The explicit solution for W_{out} is given by

$$W_{out} = \mathbf{XR'} \left(\mathbf{RR'} + \mu I \right)^{-1}, \tag{3}$$

where **X** is the training data (trajectories) and **R** are the time-series of the reservoir (with fixed A and W_{in}), and **R**' denotes the transpose of **R**. Thus, the prediction is given by

$$\hat{x}(t + \Delta t) = W_{out} r(t + \Delta t). \tag{4}$$

During the prediction phase, $\hat{x}(t)$ is used in equation (2) instead of x(t) to generate the reservoir update; thus, the reservoir becomes an autonomous system. We do not use a non-linear transformation of the reservoir in this paper.

Reservoir parameters. We use the reservoir with the size D=200 and sparsity s=90%. We also verified that reservoirs with sparsity 45% and 20% lead to similar results. The spectral radius is $\lambda_{res}=0.5$. The input layer is generated from a uniform distribution $W_{in} \sim Unif[-w,w]$ with w=5. The regularization parameter is $\mu=0.001$. The size of the training data is 1,000,000. For the prediction phase, we warm up the reservoir for 100 steps Δt .

3 Numerical Results

In this section, we present several numerical results comparing the behavior of the ESN with the simulations of the LV model.

Generalized Synchronization An interesting aspect of reservoir computing as described above is that the reservoir is never trained. Furthermore, RC has proven to be as skillful or more skillful than a number of other more sophisticated machine learning techniques.

Let

$$\frac{d\mathbf{x}(t)}{dt} = \mathbf{F}_x\left(\mathbf{x}(t)\right)$$

represent the dynamical system underlying the data; here $\mathbf{F}_x(\mathbf{x}(t))$ can be assumed unknown. Next, since the reservoir is forced by input $\mathbf{x}(t)$, the dynamics of the reservoir are non-autonomous and may be represented as

$$\frac{d\mathbf{r}(t)}{dt} = \mathbf{F}_r\left(\mathbf{r}(t), \mathbf{x}(t); \boldsymbol{\theta}\right).$$

Generalized synchronization (GS) is said to occur between these two dynamical systems when they behave in such a way that there is a functional relationship between their states. That is GS occurs if asymptotically (meaning after finite transients), $\mathbf{r}(t) = \psi(\mathbf{x}(t))$, where ψ is some unknown nonlinear transformation. In other words, the state of the reservoir becomes a deterministic function of the driver $\mathbf{x}(t)$. Unlike identical synchronization, GS does not require state equivalence, allowing complex interdependencies.

In [23] it was proposed that predictive GS occurs when $\mathbf{x} = \phi(\mathbf{r})$ without assuming $\phi = \psi^{-1}$ globally. As such, with the predictive GS, the non-autonomous dynamics of the reservoir above can be approximated in an autonomous fashion as

$$\frac{d\mathbf{r}(t)}{dt} = \mathbf{F}_r\left(\mathbf{r}(t), \tilde{\boldsymbol{\phi}}(\mathbf{r}(t)); \boldsymbol{\theta}\right).$$

The auxiliary test in the present context amounts to creating two copies of a reservoir (so that their connectivity is the same) and subjecting the two reservoirs to the same input (driver dynamical system). The only difference between the reservoir systems is that their initial states are slightly different: $\mathbf{r}_2(0) = \mathbf{r}_1(0) + \epsilon N(0,1)$. GS is validated if $\mathbf{r}_2(t) - \mathbf{r}_1(t)$ decays asymptotically to 0. This amounts to saying that the predictions must be independent of the initial conditions of the reservoir.

Testing the Independence on Initial Conditions. Since we warm up the reservoir, we test whether the reservoir becomes independent of initial conditions during the warm-up phase. To this end, after W_{in} and A are generated, we consider two reservoirs with different initial conditions. We use the initial condition $r_1(0) = 0$ for the first reservoir. The second reservoir is initialized using a normal distribution $r_2(0) = \epsilon \times N(0,1)$. Then, the two reservoirs receive the identical input x(t) (generated by the LV model) and should synchronize. Algorithm 1 describes this test. We use $\epsilon = 0.01$ and confirm that the two reservoirs synchronize for several W_{in} and A, including sparsity 45% and 20% for the connectivity matrix A. Results are presented in Figure 1 (the Log of the L^2 norm is plotted). We observe a fast exponential decay indicating that the two reservoirs synchronize by the time-step k = 20.

Algorithm 1 Testing Independence of the Reservoir on Initial Conditions

```
Generate W_{in} and A Reservoir 1: r_1(0) = 0 Reservoir 2: r_2(0) = \epsilon \times N(0,1) M=50 L2norm[0] = ||r_1(0) - r_2(0)||_2 for k=1:M do r_1(t + \Delta t) = f(Ar_1(t) + W_{in}x(t)) r_2(t + \Delta t) = f(Ar_2(t) + W_{in}x(t)) L2norm[k] = ||r_1(t + \Delta t) - r_2(t + \Delta t)||_2 end for
```

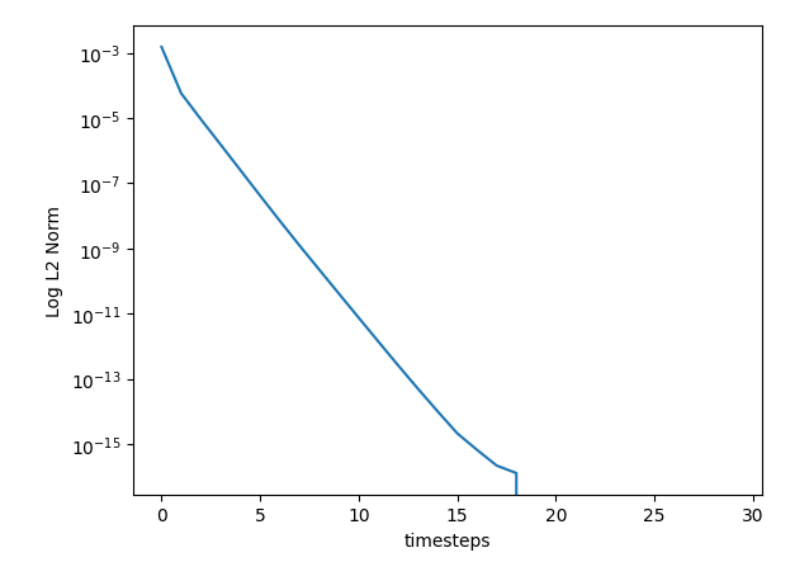


Figure 1: Log of the L^2 norm $||r_1(t)-r_2(t)||_2$ between two reservoirs with different initial conditions. One time-step is $\Delta t = 2$. We observe a fast exponential decay of the L^2 norm, indicating that the initial conditions are not affecting the utility of predictions for individual trajectories.

Time-series prediction. An example of how the ESN predicts individual trajectories is depicted in Figure 2. This trajectory is generated by the LV system in (1) with some random initial conditions and then predicted by the ESN. We observe that the ESN can predict individual trajectories for a long time. In particular, Figure 2 indicates that ESN can predict individual trajectories for approximately 8 Lyapunov times. Moreover, the ESN generates trajectories with the time-step $\Delta t = 2$, which yields a significant acceleration compared to the computational time-step of the LV model $\delta t = 0.01$.

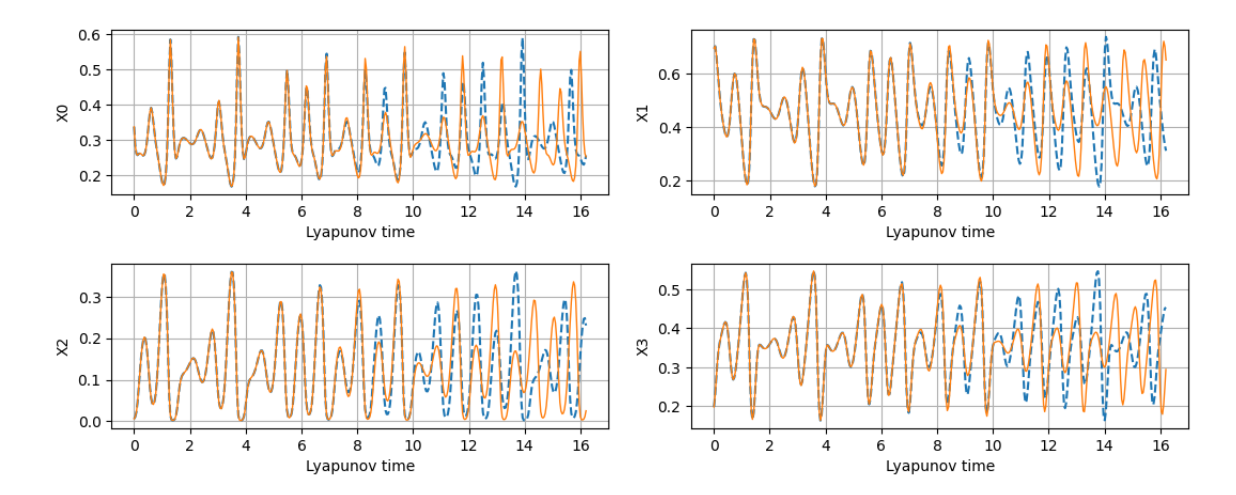


Figure 2: Prediction of individual time-series with $\Delta t = 2$. This demonstrates that the ESN predicts trajectories of the LV system for approximately 8 Lyapunov times.

Histogram prediction. Since the LV equations are a chaotic system, it is unrealistic to expect that the ESN would predict a chaotic LV trajectory forever. This is confirmed in Figure 2. However, we can ask two important questions regarding the long-time simulations of the ESN: (i) whether ESN is stable for all times, and (ii) does ESN reproduce the statistical properties of the attractor in long simulations?

We verified numerically that the ESN does not blow up and does not collapse to a steady state in long-time simulations. Moreover, the ESN can generate trajectories that correctly represent the chaotic attractor of the LV model. Figure 3 depicts that ESN correctly reproduces histograms for all four variables with a very high accuracy; the two histograms (LV and ESN) almost completely overlap everywhere. All four histograms appear to have finite tails with well-pronounced cut-offs. Variable x_0 has a much longer, slowly-decaying right tail. Zoom-in on histograms' tails is presented in the supplementary material.

Next, we perform a quantitative comparison by computing the maximum over q points in the trajectory, and fitting the Generalized Extreme Value (GEV) distribution. The GEV distribution is a three-parameter distribution with the probability density function

$$f(x) = \frac{1}{\sigma}t(x)^{\xi+1}e^{-t(x)}, \quad t(x) = \begin{cases} \left[1 + \xi\left(\frac{x-\mu}{\sigma}\right)\right]^{-1/\xi} & \xi \neq 0\\ \exp\left(\frac{x-\mu}{\sigma}\right) & \xi = 0. \end{cases}$$

Here, the three parameters are location μ , scale σ , and shape ξ . The shape parameter characterizes the tail of the distribution, and there are three distinct cases (Fisher–Tippett–Gnedenko theorem): (i) Fréchet distribution when $\xi > 0$ (heavy tails, e.g., t-student with small degrees of freedom), (ii) Gumbel distribution when $\xi = 0$ (light-tailed, e.g. exponential, normal), and (iii) Weibull distribution when $\xi < 0$ (finite-tails, e.g. uniform).

Thus, after a long stationary trajectory is generated, the maximum is computed over non-overlapping windows, i.e.

$$y_i(p) = \max_{pq \le j < (p+1)q} x_i(j\Delta t), \qquad p = 0, \dots, M - 1,$$
 (5)

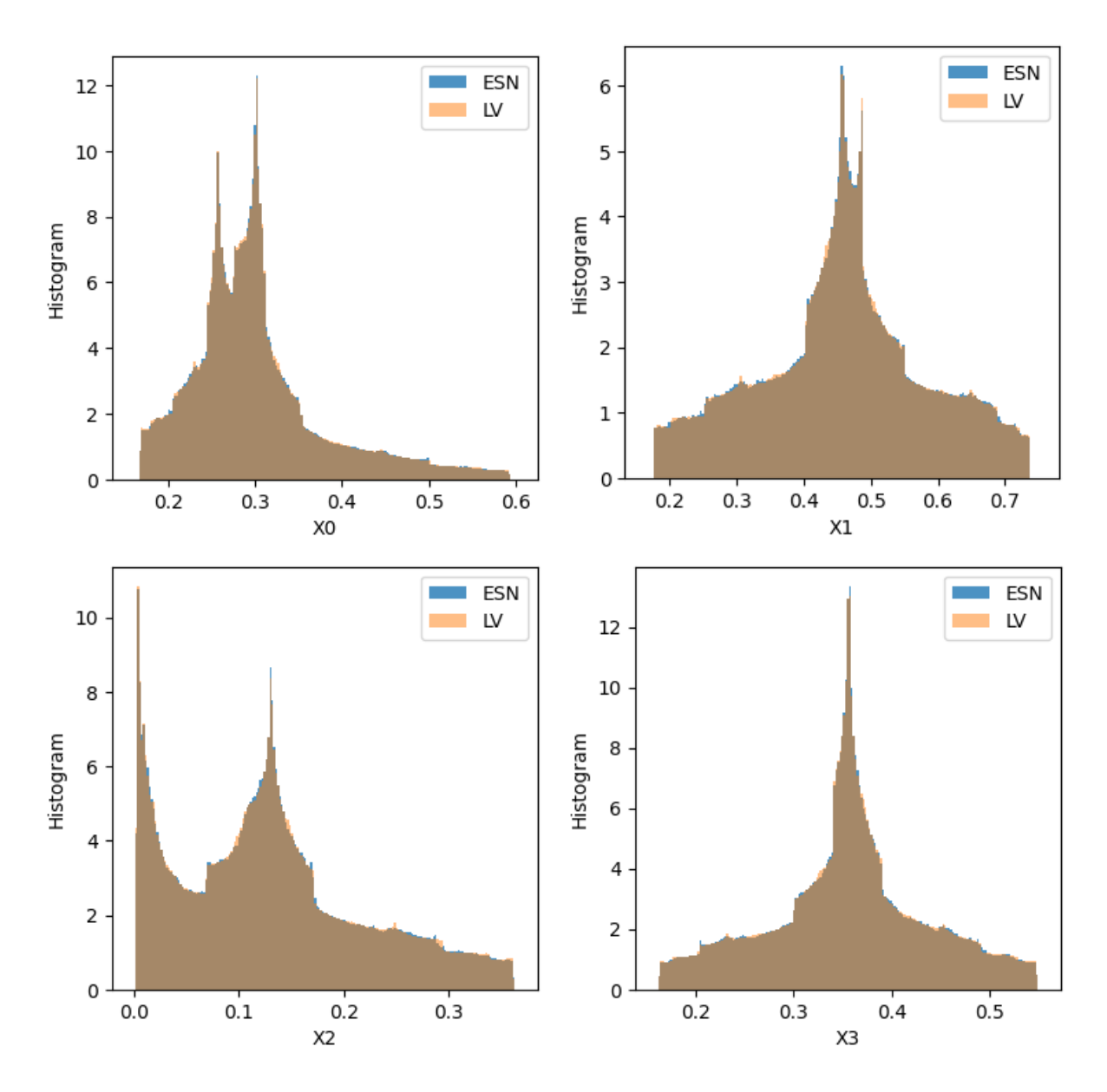


Figure 3: Histograms of dependent variables x_i , i = 0, ..., 3 in long simulations of the LV model in (1) and simulations of the ESN. There is a perfect overlap between the histogram generated by the LV system in (1) and predicted by the ESN. Zoom-in on the tails of these histograms is presented in Figure 4.

	q = 50			q = 100			q = 200		
	LV	ESN	Err	LV	ESN	Err	LV	ESN	Err
x_0	-0.925	-0.911	1.5%	-0.867	-0.847	2.3%	-0.86	-0.834	3.0%
x_1	-1.073	-1.068	0.5%	-0.937	-0.923	1.6%	-0.901	-0.891	1.0%
x_2	-1.095	-1.077	1.7%	-1.109	-1.082		-1.15	-1.099	4.5%
x_3	-1.068	-1.06	0.7%	-1.055	-1.067	1.2%	-1.089	-1.061	2.6%

Table 1: Shape parameter ξ for the GEV fit for right tails of histograms using max values computed with (5).

and $y_i(p)$, p = 0, ..., M - 1 are used for the GEV fit. The GEV fit can depend on the number of points in the averaging window, q. Recall that the sampling time-step is $\Delta t = 2$. We present three cases with q = 50, 100, and 200. This corresponds approximately to 2, 4, and 8 Lyapunov times. Results of the GEV fit are presented in Table 1. We use the Maximum Likelihood estimators implemented in scipy.stats Python package. Results in Table 1 indicate that the GEV fit is only weakly sensitive to the number of averaging points, q. The GEV fit for x_0 is influenced by the number of averaging points, q, slightly more compared to other variables. This is due to a long right tail of the histogram for x_0 (top left part of Figure 3). For all four variables, the GEV fit indicates finite tails, and there is a very good agreement between the simulations of the LV system and the trajectories generated by the ESN. Thus, the results of the GEV fit provide quantitative validation that the ESN learns the chaotic attractor of the LV system very well. In particular, the ESN reproduces the statistics of rare events for all four variables.

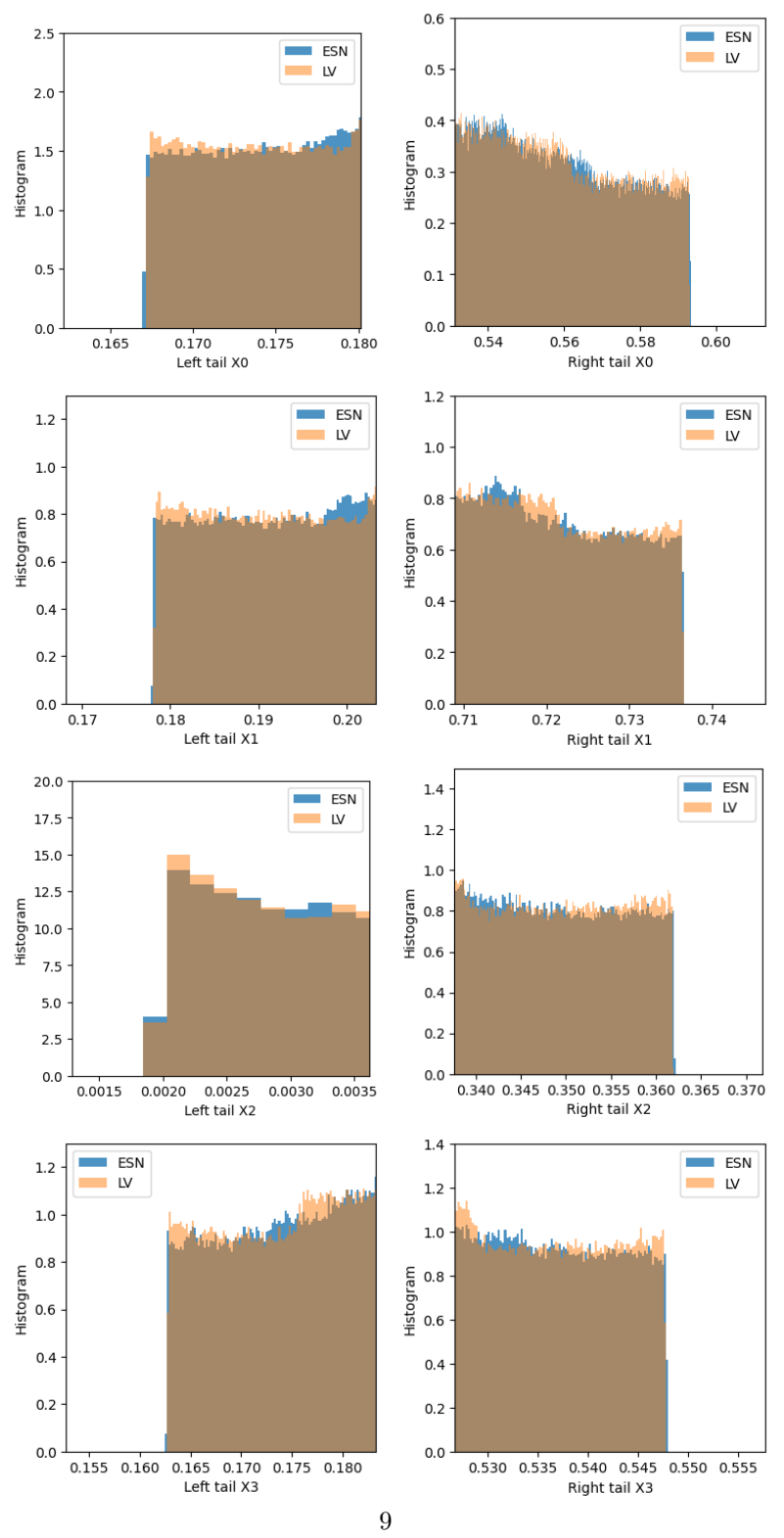


Figure 4: Zoom-in on tails of the histograms in Figure 3.

4 Conclusions

We use a standard Echo-State Network to reproduce the behavior of the 4D competitive Lotka-Volterra (LV) equation in the chaotic regime. The statistical behavior of this model is quite different from the "classical" examples such as the Lorenz-63 (L63) and the Kuramoto-Sivashinsky (KS) equations. In particular, the LV model has finite fat tails compared to fast-decaying tails of the L63 and the KS. Although both the L63 and the KS models have absorbing balls, histograms' tails in these two systems decay much faster compared to the LV model; in fact, numerically it appears that tails in the L63 and the KS decay exponentially. Therefore, the LV model provides an interesting test case to analyze how well ESN can learn attractors of chaotic systems and reproduce rare events.

It is not surprising that ESN reproduces individual time series for a long time (8 Lyapunov times in this case). The ESNs' ability to reproduce chaotic time series has been demonstrated for several chaotic systems. In addition to reproducing chaotic time series of the 4D LV model, we also demonstrate that the ESN is able to learn the underlying chaotic attractor and reproduce its statistical properties with high accuracy. We use the Generalized Extreme Value distribution to quantitatively demonstrate that ESN reproduces histograms' tails and rare events with high accuracy as well. Thus, time series generated by the ESN are, essentially, statistically indistinguishable from chaotic time series of the 4D LV model. Thus, our study provides supporting evidence that ESNs can be used in problems where it is necessary to generate trajectories with given statistical properties. Potential applications include climate studies and heat bath reservoirs.

Numerical code and data that support the findings of this study are openly available in [6].

Author Contribution

A.E.: code development, simulations, visualization. B.N.: conceptualization, manuscript writing. I.T.: conceptualization, initial code development, student supervision, manuscript writing, final draft.

Acknowledgments

A.E. acknowledges support from the UH Provost's Undergraduate Research Scholarship (PURS) and the UH Summer Undergraduate Research Fellowship (SURF). The authors thank Dr. M. Nicol for helpful discussions about the generalized extreme value distribution.

References

- [1] P. Antonik, M. Gulina, J. Pauwels, and S. Massar, *Using a reservoir computer to learn chaotic attractors, with applications to chaos synchronization and cryptography*, Physical Review E, 98 (2018), p. 012215.
- [2] W. A. S. Barbosa and D. J. Gauthier, Learning spatiotemporal chaos using next-generation reservoir computing, Chaos: An Interdisciplinary Journal of Nonlinear Science, 32 (2022), p. 093137.
- [3] M. Buehner and P. Young, A tighter bound for the echo state property, IEEE Transactions on Neural Networks, 17 (2006), pp. 820–824.

- [4] X. Chen, B. T. Nadiga, and I. Timofeyev, *Predicting shallow water dynamics using echo-state networks with transfer learning*, GEM-International Journal on Geomathematics, 13 (2022), p. 20.
- [5] N. A. K. Doan, W. Polifke, and L. Magri, *Physics-informed echo state networks*, Journal of Computational Science, 47 (2020), p. 101237.
- [6] A. Erofeev, Application of Echo-State Networks to the 4D Lotka-Volterra system; https://github.com/nepodhodish/ESNLV.
- [7] D. ESTÉVEZ-MOYA, E. ESTÉVEZ-RAMS, AND H. KANTZ, Echo state networks for the prediction of chaotic systems, in International Workshop on Artificial Intelligence and Pattern Recognition, Springer, 2023, pp. 119–128.
- [8] M. Gandhi and H. Jaeger, Echo state property linked to an input: Exploring a fundamental characteristic of recurrent neural networks, Neural Computation, 25 (2013), pp. 671–696.
- [9] M. GIRVAN, E. Ott, and B. R. Hunt, Separation of chaotic signals by reservoir computing, Chaos: An Interdisciplinary Journal of Nonlinear Science, 30 (2020), p. 023123.
- [10] A. M. González-Zapata, E. Tlelo-Cuautle, B. Ovilla-Martinez, I. Cruz-Vega, and L. G. De la Fraga, Optimizing echo state networks for enhancing large prediction horizons of chaotic time series, Mathematics, 10 (2022), p. 3886.
- [11] F. HEYDER AND J. SCHUMACHER, Echo state network for two-dimensional turbulent moist rayleigh-bénard convection, Phys. Rev. E, 103 (2021), p. 053107.
- [12] H. Jaeger, The "echo state" approach to analysing and training recurrent neural networkswith an erratum note, Bonn, Germany: German National Research Center for Information Technology GMD Technical Report, 148 (2001), p. 13.
- [13] —, Adaptive nonlinear system identification with echo state networks, in Advances in Neural Information Processing Systems, S. Becker, S. Thrun, and K. Obermayer, eds., vol. 15, MIT Press, 2002.
- [14] —, Echo state network, scholarpedia, 2 (2007), p. 2330.
- [15] H. Jaeger and H. Haas, Harnessing nonlinearity: Predicting chaotic systems and saving energy in wireless communication, Science, 304 (2004), pp. 78–80.
- [16] Y. Li and Y. Li, Predicting chaotic time series and replicating chaotic attractors based on two novel echo state network models, Neurocomputing, 491 (2022), pp. 321–332.
- [17] Z. Lu, B. R. Hunt, and E. Ott, Attractor reconstruction by machine learning, Chaos: An Interdisciplinary Journal of Nonlinear Science, 28 (2018), p. 061104.
- [18] W. Maass, T. Natschläger, and H. Markram, Real-time computing without stable states: A new framework for neural computation based on perturbations, Neural Computation, 14 (2002), pp. 2531–2560.
- [19] B. T. Nadiga, Reservoir computing as a tool for climate predictability studies, Journal of Advances in Modeling Earth Systems, (2021), p. e2020MS002290.

- [20] J. PATHAK, B. HUNT, M. GIRVAN, Z. Lu, AND E. Ott, Model-free prediction of large spatiotemporally chaotic systems from data: A reservoir computing approach, Physical Review Letters, 120 (2018), p. 024102.
- [21] J. PATHAK, Z. LU, B. R. HUNT, M. GIRVAN, AND E. OTT, Using machine learning to replicate chaotic attractors and calculate lyapunov exponents from data, Chaos: An Interdisciplinary Journal of Nonlinear Science, 27 (2017).
- [22] J. A. Platt, S. G. Penny, T. A. Smith, T.-C. Chen, and H. D. Abarbanel, A systematic exploration of reservoir computing for forecasting complex spatiotemporal dynamics, Neural Networks, 153 (2022), pp. 530–552.
- [23] J. A. Platt, A. Wong, R. Clark, S. G. Penny, and H. D. I. Abarbanel, *Robust forecasting using predictive generalized synchronization in reservoir computing*, Chaos: An Interdisciplinary Journal of Nonlinear Science, 31 (2021), p. 123118.
- [24] A. RACCA AND L. MAGRI, Robust optimization and validation of echo state networks for learning chaotic dynamics, Neural Networks, 142 (2021), pp. 252–268.
- [25] J. C. Sprott, Elegant Chaos: Algebraically Simple Chaotic Flows, World Scientific, 2010.
- [26] G. Tanaka, T. Yamane, J. B. Héroux, R. Nakane, N. Kanazawa, S. Takeda, H. Numata, D. Nakano, and A. Hirose, *Recent advances in physical reservoir computing: A review*, Neural Networks, 115 (2019), pp. 100–123.
- [27] J. A. VANO, J. C. WILDENBERG, M. B. ANDERSON, J. K. NOEL, AND J. C. SPROTT, Chaos in low-dimensional Lotka-Volterra models of competition, Nonlinearity, 19 (2006), p. 2391.
- [28] P. VLACHAS, J. PATHAK, B. HUNT, T. SAPSIS, M. GIRVAN, E. OTT, AND P. KOUMOUT-SAKOS, Backpropagation algorithms and reservoir computing in recurrent neural networks for the forecasting of complex spatiotemporal dynamics, Neural Networks, 126 (2020), pp. 191–217.
- [29] R. Wang and D. Xiao, Bifurcations and chaotic dynamics in a 4-dimensional competitive Lotka-Volterra system, Nonlinear Dyn, 59 (2010), p. 2391.
- [30] I. B. YILDIZ, H. JAEGER, AND S. J. KIEBEL, Re-visiting the echo state property, Neural Networks, 35 (2012), pp. 1–9.